KATO, K. (1967). Privatmitteilung. Mineralog.-Petrogr. Inst. Hamburg.
KETELAAR, J. A. A. (1964). *Chemische Konstitution*. Braunschweig: Verlag Vieweg.
KITAIGORODSKI, A. J. (1961). *Organic Chemical Crystallography*. New York: Consultants Bureau.
KRAEFT, U. (1967). *Naturwissenschaften*, **54**, 441.
LAI, T. F. & MARSH, R. E. (1967). *Acta Cryst.* **22**, 885.
PAULING, L. (1962). *Die Natur der chemische Bindung*. Weinheim: Verlag Chemie.
PEDERSEN, B. F. & PEDERSEN, B. (1965). *Tetrahedron Letters*, No. 34, 2295.
STUART, H. A. (1967). *Molekülstruktur*. S. 95. Berlin-Heidelberg-New York: Springer Verlag.
SUBRAMANIAN, E. (1966). *Z. Kristallogr.* **123**, 222.
WALTER, W. & MAERTEN, G. (1963). *Liebigs Ann.* **669**, 66.
WALTER, W., MAERTEN, G. & ROSE, H. (1966). *Liebigs Ann.* **691**, 25.
X-ray 63 Program-System (1963). Univs. of Washington and Maryland.

Acta Cryst. (1969). B**25**, 275

The Defect Structure of $Fe_{1-x}O$

BY F. KOCH* AND J. B. COHEN

Department of Materials Science, The Technological Institute, Northwestern University, Evanston, Illinois U.S.A.

(*Received* 1 *February* 1968)

The superstructure peaks first reported by Manenc in quenched specimens of $Fe_{1-x}O$ have been studied in detail, with a single crystal of $Fe_{0.902}O$. These peaks were found to be due to periodically spaced clusters of vacancies, each cluster of neighboring octahedral cation sites being grouped about occupied tetrahedral cation sites. The clusters do not appear to be regions of magnetite. Structure factor calculations, based on a model where each cluster consisted of 13 vacancies and 4 tetrahedral ions, give substantial agreement with the observed intensities. Small displacements towards this cluster are found for the surrounding cations while displacements in the opposite sense are found for anions. The basic cluster persists at temperatures in the one phase field, up to at least 1150°C and to a value of $x = 0.082$, although the long-range periodicity of the clusters is destroyed.

Introduction

The 'ideal' structure of $Fe_{1-x}O$ (known in mineral form as wüstite) is that of rocksalt (NaCl), Strukturbericht type $B1$ (Wyckoff & Crittenden, 1925). The phase is stable only above about 570°C and although there are large variations in x, the stoichiometric composition, FeO, apparently does not exist at normal pressures (Darken & Gurry, 1945). The deviation from stoichiometry results from vacancies on cation sites (Jette & Foote, 1933), and some of the tetrahedral sites are occupied by cations (Roth, 1960; Smuts, 1966). Despite this detail, there remains one major question – how the vacancies and tetrahedral ions are arranged. Thermodynamic measurements suggest that this arrangement is not random for certain regions of the one phase field (Humphrey, King & Kelley, 1952; Brynestad & Flood, 1958; Salmon, 1961), as do measurements of conductivity (Bransky & Tannhauser, 1967; Swaroop & Wagner, 1967). Recent measurements of the chemical diffusion coefficient by Hembree & Wagner (1966) indicate that as the deviation from stoichiometry increases, the chemical interdiffusion coefficient decreases, rather than increasing as would be expected if random vacancies were being produced.

Manenc and co-workers in a series of papers (1963*a*, *b*; 1964) have shown that there are weak diffraction peaks from quenched $Fe_{1-x}O$ in addition to those expected from a $B1$ structure. One set of these peaks (to be referred to as satellite peaks) corresponds to a repeat distance of 100–500 Å and was attributed to a periodic mixture of two phases, differing in vacancy content, initiated during quenching and further developed in subsequent heat treatments. This periodic two-phase structure was directly observed in the electron microscope. A second set of extra peaks (referred to as superstructure peaks here) is present even for $x \geq 0.08$ when only one phase is observed; these correspond to a cubic unit cell *about* 2·5 times the dimensions of that for $Fe_{1-x}O$ and were attributed to $Fe_{1-x}O$ with ordered vacancies.

There are two opposing schools of thought on the type of defect arrangement which might be expected. On the one hand, Bertaut (1953) has shown that the lattice energy of a nonstoichiometric compound such as $Fe_{1-x}O$ is greatly reduced, relative to a random structure, by ordering cation vacancies in such a way that their spacing is as great as possible. This provides a basis for understanding why there are ordered vacancies in $Fe_7S_8(Fe_{0.875}S)$. On the other hand, there are a number of reasons for suspecting that the vacancies are clustered together in small regions locally similar to Fe_3O_4. Since the oxygen ions are approximately in

* Presently on the Technical Staff of the Bell Telephone Laboratories, Murray Hill, New Jersey, U.S.A.

face centered cubic close packing in both the spinel structure of Fe_3O_4 and in $Fe_{1-x}O$, the important difference is in the arrangement of iron ions on the available octahedral and tetrahedral sites. Interactions between tetrahedral and octahedral cations play a major role in establishing the spinel structure and probably have a similar importance in $Fe_{1-x}O$. As Bertaut considered only interactions between filled and vacant *octahedral* sites, it would not be surprising to find his conclusions were not applicable to the Fe–O system.

The similarity in ion arrangement in $Fe_{1-x}O$ and Fe_3O_4 suggests that each unit cell of Fe_3O_4 can be compared to a cube, two FeO cells on each edge. Indeed, a plot of twice the lattice parameter of $Fe_{1-x}O$ *versus* vacancy concentration extrapolates to $Fe_{0.75}O$ at about the lattice parameter of the spinel (Jette & Foote, 1933). The heats of formation of Fe_3O_4 (but based on a formula $Fe_{0.75}O$) and $Fe_{1-x}O$ differ only slightly (Darken & Gurry, 1945). Magnetic measurements show there is little change of the Néel temperature of $Fe_{1-x}O$ with x (Koch & Fine, 1966). This result can best be understood if the vacancies are clustered together so that most iron ions are in the local environment of stoichiometric FeO. If single vacancies are ordered on a sublattice, large changes in the Néel temperature with x are expected. The clustering of vacant sites is also indicated by the shifted magnetic hysteresis loop found by Roth (1959) and confirmed by Koch & Fine. [Roth pointed out that some of his neutron diffraction data supported such local arrangements. He worked with quenched powders, and one of the sources for this suggestion was his observation of a weak diffuse scattering in the vicinity of peaks from Fe_3O_4; however, $Fe_{1-x}O$ is quite ductile and we have found that any deformation (even rapid quenching) greatly broadens the superstructure peaks found by Manenc *et al.* (1963). The positions of the broad peaks found by Roth are closer to the positions of these extra peaks than to Fe_3O_4 peaks.]

It is obviously important to establish whether any configurations which may be inferred from measurements on quenched samples really persist in the one-phase field for certain compositions and temperatures where the studies of thermodynamic properties, conductivity, and diffusivity have actually been made.

In this paper, a structural investigation of $Fe_{1-x}O$ is reported. Octahedral cation vacancies are found to be clustered in groups, with tetrahedral iron ions within each cluster; these clusters are periodically arranged in quenched specimens. Although the clusters *do* exist at high temperatures, their periodicity is largely lost. The cation arrangement resembles Fe_3O_4 in some ways, but some important differences will be shown.

Experimental procedures

Most samples were prepared from Fe supplied with a nominal purity of 99·999 percent although spectrographic analysis indicated there might be as much as 0·07 weight percent of substitutional impurities. Specimens were prepared in a vertical tube furnace by suspending a carefully cleaned and weighed sample of iron on a Pt wire. The premixed and dried CO/CO_2 gases (chosen to give the desired composition as indicated by the results of Darken & Gurry) flowed upwards in the furnace past the sample at a flow rate adjusted to avoid thermal diffusion gradients in the gas, as suggested by Darken & Gurry. The composition of the $Fe_{1-x}O$ product was checked by measuring the weight change of a specimen and good agreement with the results of Darken & Gurry was obtained in all cases. Equilibrium was insured by allowing at least enough time at temperature for the average composition to be within 0·01 percent of the final composition. (These times were estimated from the known geometry of the specimen and the recent diffusivity measurements of Hembree & Wagner.) The samples were quenched by either pulling them into the cold zone of the furnace, or with a blast of cold helium.

In addition to measurements on quenched samples, some qualitative measurements were made at high temperatures under equilibrium conditions using the M.R.C.* high temperature attachment to the G. E. diffractometer and a Pt – 40 percent Rh ribbon heater. A coarse grained specimen was made *in situ* in the attachment by spot welding a small sheet of iron to the heater and equilibrating in an appropriate flowing CO/CO_2 mixture. $Fe_{1-x}O$ recrystallizes at 1100 °C in millimeter-size grains with {001} planes parallel to the surface (Manenc *et al.* 1963*a*) so that very strong 002 and 004 peaks can be obtained from one grain by some minor adjustment of a specimen's orientation at temperature. Room temperature measurements of the lattice parameter of powder specimens prepared in this way indicated that the compositions were those expected from the gas ratio employed; the parameters used by Levin & Wagner (1963) were used for this comparison. The temperature was measured with a Pt – Pt 10 percent Rh thermocouple welded to the back of the heater ribbon. There could be large gradients across the sample due to the fact that the oxide is not a good thermal conductor, so the values were checked on a dummy specimen by opening the camera at temperature so that an optical pyrometer could be sighted on the surface. In the range of measurements (800–1200 °C), this measurement indicated that the surface was at most 75–125 °C lower in temperature than the heater ribbon. All X-ray lines were reasonably sharp, so the gradient in the plane of the surface was small. Temperature was controlled to about ± 5 °C, with a Thermac–Labac controller. The known phase boundaries for $Fe_{1-x}O$ could *not* be used to calibrate the furnace, since large hysteresis was found for the reactions at these boundaries. Spectrographic analysis after a high temperature run indicated that no Pt or Rh from the heater was incorporated by the specimens, within a detection limit of 1 p.p.m.

* Materials Research Corp., Orangeburg, New York

For the above experiments monochromatic Co $K\alpha$ radiation was used with a doubly bent LiF crystal (Schwartz, Morrison & Cohen, 1964).

Single-crystal measurements were made on a slab (0·17 cm × 0·11 cm × 0·02 cm) cleaved from a large grain within a specimen prepared by Levin & Wagner. While this geometry effectively limited the available diffraction peaks to those obtained by reflection from the large {100} cleavage faces, a more suitable geometry could not be obtained because of the tendency of this material to deform during grinding. The starting material for this crystal was zone refined iron (99·986 percent Fe) supplied by the Battelle Memorial Institute. This was equilibrated in a CO/CO_2 mixture of ratio $\frac{2}{3}$, at 1000 °C, resulting in a sample of $Fe_{0.902}O$ as established by the increase of weight on oxidation. Diffracted intensities from this single crystal were measured on the G. E. diffractometer with a quarter-circle Eulerian cradle. The integrated intensities were obtained from the area under chart recordings of the peaks made in $\theta - 2\theta$ scans. The precision of this integration, checked over a wide range of intensities with the scaler, was ±10 percent. Receiving slits were opened sufficiently to make the integrated intensity of a high angle peak independent of slit size. Measurements were made both with filtered Mo $K\alpha$ radiation and monochromatic Co $K\alpha$ radiation. The detector was a scintillation counter with a pulse height analyzer.

It is essential to avoid the formation of a second phase in preparing quenched samples. The measurements on the single crystal were made with a composition ($x = 0{\cdot}098$) that should have consisted entirely of the ordered phase of $Fe_{1-x}O$. If the periodic two-phase mixture described by Manenc had not been avoided, the $B1$ peaks would have appeared broad due to the set of nearby satellites, whereas these peaks were in fact sharp. (This broadening was observed with some specimens of other compositions.) To check on possible decomposition into Fe_3O_4 and/or Fe, the saturation magnetization of a portion of the same specimen from which the single crystal was obtained was measured in a vibrating sample magnetometer (Koch, 1967). The measured moment of 0·028 e.m.u./g. corresponded to only a very small amount (0·03 weight percent) of precipitated Fe_3O_4. No diffraction peaks from Fe_3O_4 or Fe were seen [with a detection limit of about 0·1 percent from any sharp peaks from Fe_3O_4; this phase forms with cube axes parallel to those of $Fe_{1-x}O$ (Manenc, 1963*a*)]. Some transmission electron microscopy and electron diffraction studies were performed on a Hitachi HU-11A microscope. Specimens were thinned and electropolished in flowing phosphoric acid held at 90 °C. The periodic two-phase mixture observed by Manenc was not seen although diffraction peaks did appear which were apparently the result of a thin film of Fe_3O_4 formed on the surface. In addition, the superstructure peaks observed with X-rays were readily apparent in the electron diffraction patterns.

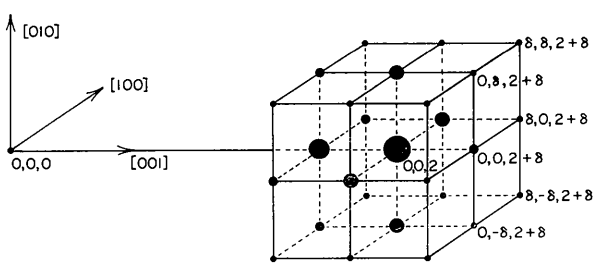

Fig. 1. Superstructure peaks observed around the 002 fundamental peak. The size of each dot represents the intensity.

Qualitative results with quenched crystals

The superstructure peaks observed around each $B1$ peak with quenched single crystals or coarse-grained specimens are indicated schematically in Fig. 1. Note that the pattern cannot be due to one-dimensional periodicities in directions of the form ⟨100⟩ in different parts of the crystal. Some additional peaks such as $0,0,4 - 2\delta$ and $0,0,4 - 3\delta$ were observed although the $0,0,2 - 2\delta$ peak was never seen. The $0,0,\delta$ peak near the origin was sometimes present, but was very weak. The pattern shown in Fig. 1 also occurred around the equivalent 200 and 020 peaks. This was checked with precession films and electron diffraction patterns. Sheets of weak diffuse scattering were present on reciprocal lattice planes such as h, k, 2-δ. The intensities of the various superstructure peaks relative to each other were about the same for a number of quenched specimens of the same composition but because these comparisons were made on coarse grained specimens, not single crystals, nothing can be said of the absolute intensities from specimen to specimen. The extra reflections are not due to a surface reaction; on etching one specimen to remove 50 percent of its thickness, the intensities of the peaks at $0,0,2 \pm \delta$ remained the same to within 10 percent. Neither were they due to a precipitation reaction, as aging quenched $Fe_{0.949}O$ at 250 °C only caused the superstructure peaks to disappear with time. On the other hand, Fe_3O_4 lines appeared and increased in intensity during this aging.

The strongest superstructure peak ($0,0,2 - \delta$) could be observed over a wide range of x. As Table 1 shows, the position of this peak is only slightly affected by composition, indicating that the average periodicity involved is relatively constant. The results, therefore, are not compatible with ordering of single vacancies. There is a marked broadening of the peaks as x approaches zero, which might result from a decrease in the size of any ordered regions.

As already mentioned, the extra peaks were quite sensitive to deformation by grinding, much more so than the fundamentals. Even deformation due to a helium gas quench was sufficient to broaden these. The diffuse intensity from powder samples was strikingly similar to that found by Roth (1960) with neutron

diffraction. There was no difficulty in detecting this with monochromatic Co $K\alpha$ radiation, and X-rays seem as suitable as neutrons for such studies.

Results for samples measured under equilibrium conditions at temperature

In Fig. 2 results obtained with a single grain in a coarse-grained polycrystalline specimen in equilibrium at elevated temperatures are presented. The extra lines are weaker and much broader but still present. Thus long-range order is destroyed but the local arrangement is the same at temperature in the one-phase region as in quenched samples. The intensity falls with increasing temperature (lower portion of Fig. 2); however, in a fixed CO/CO_2 environment the iron content increases slightly on increasing the temperature. The concentration was thus deliberately altered from $Fe_{0.877}O$ to $Fe_{0.918}O$ at 1150°C by altering the CO/CO_2 ratio. A decrease in the diffuse peak accompanied increasing iron content, as shown in the upper portion of Fig. 2. The values $x=0.082$ and $T=1150$°C are well within the region where Bransky & Tannhauser interpreted their measurements of conductivity as indicating only random defects. This is clearly not the case.

Fundamental reflections from a quenched single crystal of $Fe_{0.902}O$

Integrated intensities were corrected by the Lorentz-polarization factor and by an absorption factor. The absorption correction was found by measuring the intensity of fluorescent radiation for each crystal orientation used to obtain diffraction peaks. The pulse height analyzer was readjusted to accept the fluorescent Fe $K\alpha$ radiation and reject the Mo $K\alpha$ radiation used for excitation. Wavelengths close to Fe $K\alpha$ in the exciting beam were reduced by placing a 0·002 in. Zr filter over the divergence slit. (In the measurements of peak intensities, this filter was placed over the receiving slit.)

An absorption correction for each reflection was also approximated from the area of the large face of the crystal when projected in the direction of the incident and diffracted beams. Random discrepancies of up to 20 percent were noted in the two sets of absorption corrections. Those derived from the fluorescent intensities were deemed more suitable since they included the effects of small surface irregularities and also the contribution from edges and corners. Some inaccuracy in this technique is to be expected because of the difference in the absorption coefficient for the Fe $K\alpha$ and Mo $K\alpha$. For reflections from the large face,

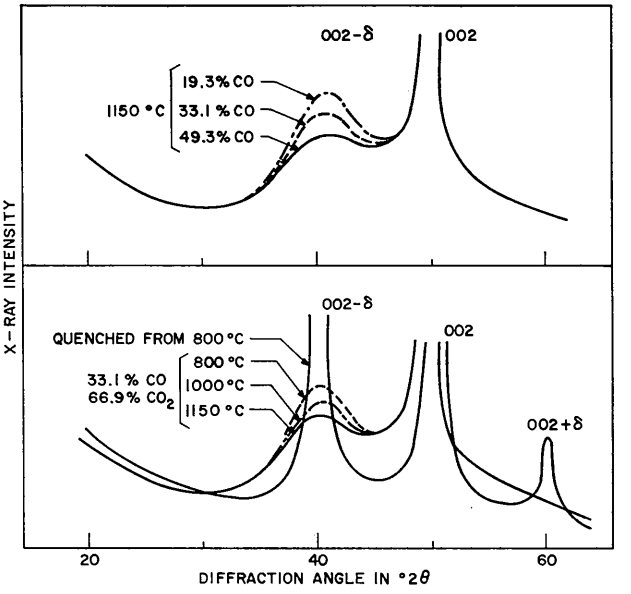

Fig. 2. Diffuse intensity measured along [001] from one grain in a coarse grain sample held under equilibrium conditions at elevated temperatures. Lower portion: results for three elevated temperatures with a 33·1 percent CO/66·9 percent CO_2 atmosphere (approximately $Fe_{0.9}O$) and after quenching this same sample from 800°C. Upper portion: fixed measuring temperature (1150°C), varying gas mixtures containing 19·3, 33·1 and 49·3 percent (balance CO_2) corresponding to $x=0.123$, 0·102, and 0·082 respectively.

Table 1. *Effect of composition on breadth and position of the supplementary peaks*

x Composition	$B^*_{(0,0,2-\delta)}$ Line breadth in °2θ	t^* Av. domain size in Å	δ	Repeat period (number of $Fe_{1-x}O$ cells
0·902	0·20	> 500	0·384	2·601
0·920	0·35	340	0·373	2·68
0·923	0·56	190	0·366	2·73
0·947	3·4 (?)	28	0·383 (?)	2·61 (?)

* $B_{(0,0,2-\delta)}$ represents the angular width of the $(0,0,2-\delta)$ peak at half maximum. To obtain roughly the broadening due to the domain size from the measured values of $B_{(0,0,2-\delta)}$, the following equation was used:

$$B^2_{(0,0,2-\delta)} = B_0^2 + B_D^2$$

Here B_D is the angular broadening due only to the size of the domains and B_0 is the instrumental breadth of a peak from an infinite perfect crystal; this was taken equal to the breadth of the narrowest observed peak (0·20°). The average domain diameter was calculated from the equation:

$$t = 0.9\,\lambda / B_D \cos\theta\,.$$

however, the corrected intensities were reliable enough to give an R value less than 0·10 for fundamental reflections, for which the structure factors were essentially independent of the detailed model for the defects (see below).

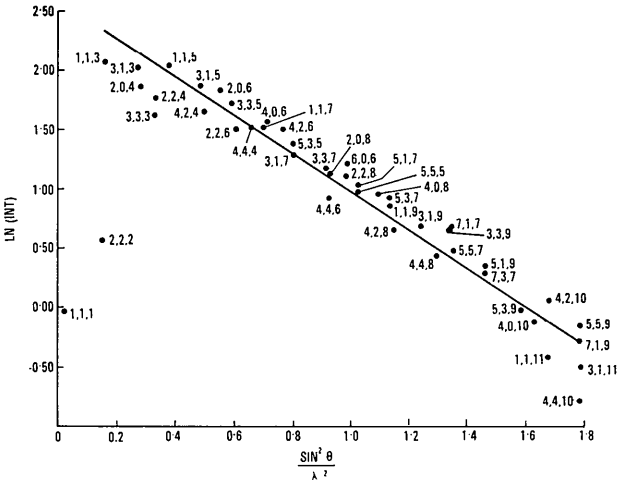

Fig. 3. $\ln[I/|F|^2]$ *vs.* $\sin^2\theta/\lambda^2$. (I is the observed intensity corrected for absorption and the Lorentz–polarization factor and F is the structure factor calculated for a $B1$ structure with an occupation factor of 0·904 for iron on octahedral sites.)

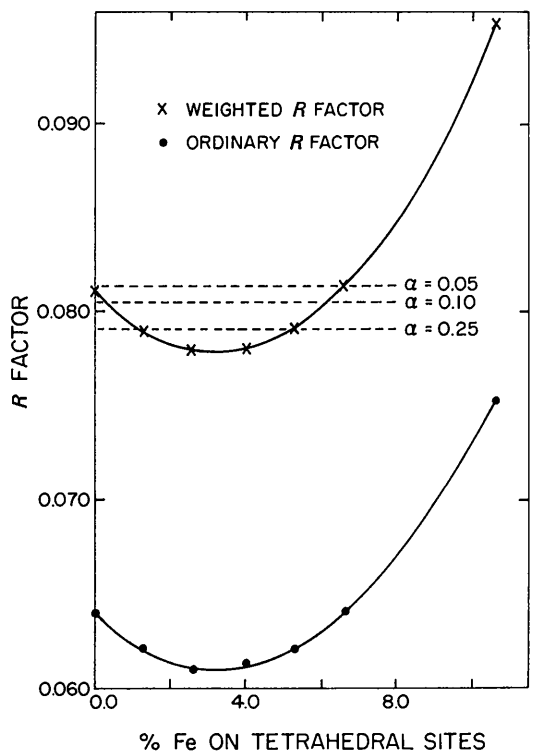

Fig. 4. Agreement between calculated and observed structure factors for fundamental peaks as a function of the amount of iron on tetrahedral sites. $R''=[\Sigma w_i(|F_o|-|F_c|)^2/\Sigma w_i|F_o|^2]^{1/2}$, and $R'=\Sigma|F_o|-|F_c|/\Sigma|F_o|$, are shown. The dotted lines indicate the maximum R'' values obtained by tests at the 95, 90 and 75 percent confidence levels ($\alpha=0{\cdot}05$, 0·1, 0·25).

The *ORFLS* computer program (Busing, Martin & Levy, 1960, as modified by Ibers, 1965) was used for structure-factor calculations and least-squares refinements. For Fe^{2+} the Hartree–Fock atomic scattering factors from *International Tables for X-ray Crystallography* were used with an anomalous dispersion correction for Mo $K\alpha$ also taken from the Tables. For Co $K\alpha$ the dispersion correction was taken from Cooper (1963). The scattering factors for O^{2-} reported by Takonomi (1965) were used without a dispersion correction.

It is convenient to discuss the analysis of the fundamental peaks first. For peaks of this type measured with Mo $K\alpha$, the agreement with what is expected from a $B1$ structure is quite good, as illustrated by the temperature factor plot shown in Fig. 3. The overall temperature factor obtained from the slope of the straight line fit was 0·79 Å², as compared to Smuts's value of $1{\cdot}03\pm0{\cdot}12$ Å². The 111, 222, and 333 peaks appear to be affected by extinction (see Fig. 3) and were not used in subsequent analysis. A listing of the observed structure factors can be found in Table 4.

The agreement for the $B1$ peaks can be improved if some iron ions are introduced on tetrahedral sites. A specific tetrahedral content was assumed and the occupation on octahedral sites adjusted to correspond with the known overall composition. Having thus specified the iron distribution, the scale factor and two isotropic temperature factors (one for oxygen ions and the other for iron ions) were refined with the least-squares program. This process was then repeated for a series of other concentrations of tetrahedral iron ions. An empirical weighting factor was used of the form:

$$W_i=a+1/F_{obs}+c/F_{obs}^2$$

(Cruickshank, 1965). The values of a and c which minimized the variation of $(F_{obs}-F_{cal})$ with F_{obs} were 1 and 6 respectively.

The effect of thus changing the tetrahedral content on the 'ordinary R index' (R') and the 'weighted R index' (R'') is shown in Fig. 4. The minimum value of R'' corresponds to about 3·3 percent of the iron on tetrahedral sites, about half to two thirds of the tetrahedral content found by Roth (1960) and Smuts for this composition. The present analysis differs from the earlier work in employing separate temperature factors for oxygen and iron. The application of a significance test as discussed by Hamilton (1965) shows that the present data for the $B1$ peaks are actually compatible with a considerable range of tetrahedral contents, which include the previous studies. In this case, the test is made against $R_{1,43-3,\alpha}$ (see Hamilton for the notation) since 43 $B1$-type reflections were included and 3 parameters were refined for each tetrahedral content. The values of R'' corresponding to $\alpha=0{\cdot}25$, 0·10 and 0·05 are shown in Fig. 4 as dotted lines (these are in effect 75, 90 and 95 percent confidence limits).

In addition to the weighting systems discussed above, similar calculations were made using weighting factors of $1/F_{obs}$. The results as regards tetrahedral occupation were essentially the same, and the temperature factors were within the standard deviations 0·03 Å² for Fe and 0·10 Å² for oxygen. The values using Cruickshank's weighting scheme were 0·79 Å² and 0·93 Å² for iron and oxygen respectively.

There seems little doubt that tetrahedral ions are present. It is gratifying to see this result in three separate investigations, one with powders using neutrons, one with powders using X-rays, and this one using X-rays and a single crystal. Further proof of tetrahedral occupation was obtained from the analysis of the superstructure peaks to be discussed below.

Analysis of superstructure peaks

An initial attempt was made to treat the superstructure lines as satellites, and to try to analyze them using Guinier's formulation (1963) in terms of a modulation of atomic displacement and scattering factor. However, quite different values were obtained from superstructure reflections near the 002 and from those near the 004. It was next decided to treat the pattern as that from a large unit cell. In doing this, we have found a partial Patterson function formed from only the superstructure peaks to be useful. Provided that the same structure factors are obtained from the fundamental peaks with the ordered and disordered structures, an interesting physical interpretation can be made of the resulting maps. This requirement is satisfied here for any rearrangement of a specified number of octahedral iron ions and also for any rearrangement of tetrahedral ions since all ions of each type will scatter in phase for fundamental reflections.

As suggested by Frueh (1953), such maps may be visualized as the Patterson function of a difference structure, formed by subtracting the electron density of a disordered crystal from the ordered structure. In general, there will be contributions both from substitutional rearrangement and from displacements with ordering. Our approach has been to disregard the displacements initially and to develop a model for the substitutional arrangement of filled and vacant sites. By considering Patterson peaks near the origin only, effects of displacements are minimized. With this simplification, we may formulate an expression for the Patterson function $P(uvw)$ in terms of the average occupation of sites separated by the vector $[uvw]$. Disregarding the scattering from the oxygen sublattice, which is completely occupied, the arrangement of the remaining cation sites may be considered as occupied by a binary AB alloy where Fe (A atoms) and cation vacancies (B atoms with scattering factor of zero) occupy the octahedral and tetrahedral sublattices. We may then express the Patterson function $P(uvw)$ in terms of the pair probabilities P_{AA}^{uvw}, P_{AB}^{uvw}, P_{BA}^{uvw}, and P_{BB}^{uvw} where the superscript uvw indicates the interatomic vector. As an example, P_{AB}^{uvw} is the probability that the uvw vector from an A atom terminates on a B atom.

$$P(uvw) = N[X_A P_{AA}^{uvw} Z_A^2 + X_A P_{AB}^{uvw} Z_A Z_B + X_B P_{BA}^{uvw} Z_B Z_A + X_B P_{BB}^{uvw} Z_B^2] .$$

Here Z_A and Z_B are atomic numbers and X_A and X_B are atomic fractions. Using the relations:

$$P_{AA}^{uvw} + P_{AB}^{uvw} = 1,\ P_{BB}^{uvw} + P_{BA}^{uvw} = 1,\ X_A P_{AB}^{uvw} = X_B P_{BA}^{uvw} ,$$

then

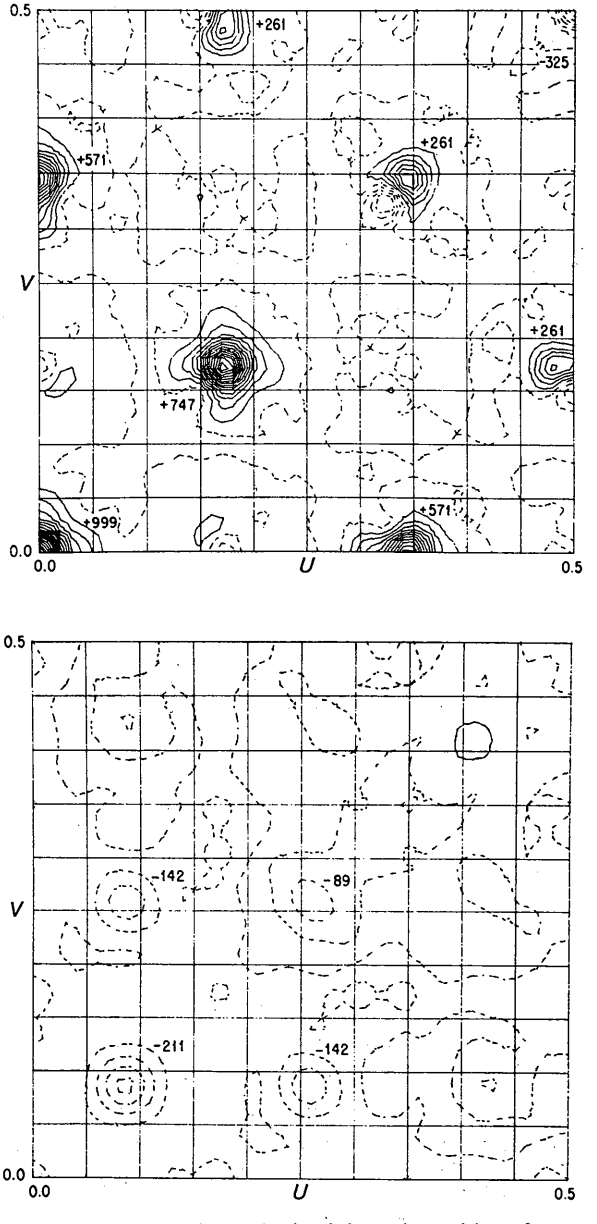

Fig. 5. Patterson sections obtained from intensities of super structure peaks. (*a*) $z=0$ (*b*) $z=\frac{1}{12}$.

$$P(uvw) = N\left[(X_A Z_A + X_B Z_B)^2 + X_A X_B (Z_A - Z_B)^2 \times \left\langle 1 - \frac{P_{AB}^{uvw}}{X_B} \right\rangle\right]. \quad (1)$$

The first term on the right is the Patterson function of the average structure which results in the fundamental reflections. The second term is the Patterson function of the extra peaks and involves deviations from a random array, as P_{AB}^{uvw} is compared to X_B – the random probability of a B atom being next to an A at the end of some vector $[uvw]$. It is clear that the first term will dominate; this is why Frueh proposed that only the superlattice peaks be used in a partial Patterson synthesis. The term in carats is nothing more than the Warren short-range order parameter, α_i, and can produce positive or negative peaks, or zero values if the arrangement of A and B is random. Quantitative values can in principle be obtained from such a plot rather simply because for $u=0$, $v=0$, $w=0$ (*i.e.* each atom with respect to itself), $P_{AB}^{uvw} \equiv 0$. The value at the origin of Patterson space can thus be used to normalize the values at other positions. The values of α can then be used to seek an initial model for refinement. If there are tetrahedral ions, equation (1) applies to those and to the lattice of octahedral sites separately, with due regard to the difference in density of lattice points. A similar formulation of Frueh's technique was proposed by Cowley (1960) and was used by Gatineau (1964) in a study of ordering Al and Si in mica.

The indexing of the superstructure peaks poses a problem. From the spacing between a superlattice reflection and a fundamental peak, the value $\delta = 0{\cdot}384$ is calculated; δ may in fact be irrational even though the extra peaks are sharp. This is interpreted to mean that the repeat distance in a [100] direction is a variable (integer) number of the $B1$ cells, from place to place in the specimen, so the observed spacing corresponds to the average (non-integer) repeat distance. A similar interpretation has been attached to the non-integer repeat distances observed in metallic alloys showing 'long period superlattices'. By calculating the diffraction from various trial arrangements, Fujiwara (1957) has shown that sharp diffraction peaks corresponding to an average periodicity *can* exist. A mixture of periodicities would be difficult to analyze. Instead, the average periodicity in the actual structure was approximated by an integral multiple of the $B1$ cell parameter. With the approximation, $\delta = 0{\cdot}333$, the extra peaks are indexed in terms of a cubic unit cell with a cell parameter three times that of the $B1$ cell (to be referred to a $3X$ cell). As an example, 002-δ is re-indexed 005 instead of 0,0,4·95. Similarly, the approximation, $\delta = 0{\cdot}400$ leads to a $5X$ cell, so 002-δ becomes 008 instead of 0,0,8·08.

Some error in the Patterson function will result from these approximations. This error can be estimated by differentiating the Patterson function with respect to the index, h:

$$\Delta P(uvw) = -\frac{2\pi u}{V_c}\left[\Sigma F_{hkl}^2 \sin 2\pi(hu+kv+lw)\right]\Delta h \,. \quad (2)$$

It is clear that: (*a*) with the two choices for δ and hence Δh, the error in the Patterson is of opposite sign so that the importance of indexing can be examined and (*b*) the effect should be quite small in any case for interatomic vectors close to the origin.

The heights of Patterson peaks obtained with the two choices for δ were quite similar, indicating that this error was indeed small. In what follows only the $3X$ cell will be shown. Fig. 5 shows two sections of the Patterson function determined for a $3X$ cell from 72 superstructure peaks measured with Mo $K\alpha$ and 43 such peaks observed with Co $K\alpha$. (The Co $K\alpha$ data were used in order to include an important contribution from the low index peaks even though the data were perhaps less reliable due to the extinction effects observed with the fundamental peaks. Maps made with estimated corrections of extinction for the Co peaks were quite similar.) An outstanding feature of these Patterson maps is the large positive peaks corresponding to the vectors $\frac{1}{6}$, $\frac{1}{6}$, 0 and $\frac{1}{3}$, 0, 0. These vectors respectively span the distances between nearest neighbor and next-nearest neighbor octahedral sites. Positive peaks will result if the neighbors of vacancies are also vacancies. Similarly, the negative peak corresponding to the vector $\frac{1}{12}$, $\frac{1}{12}$, $\frac{1}{12}$ (the vector between

Table 2. *Volume integrals of Patterson peaks*

Vector coordinates u,v,w	i	Patterson peaks from observed intensities	α_i	Patterson peaks calculated using model of substitutional order	Calculated using model of substitutional order and displacements from the model
0, 0, 0	0	1·00	1·00	1·00	1·00
$\frac{1}{2}$, $\frac{1}{2}$, 0	1	0·57	0·35	0·39	0·54
1, 0, 0	2	0·35	0·15	0·11	0·30
1, $\frac{1}{2}$, $\frac{1}{2}$	3	0·00	0·02	−0·01	0·00
1, 1, 0	4	0·06	−0·04	−0·03	0·03
$\frac{3}{2}$, $\frac{1}{2}$, 0	5	0·11	−0·25	−0·03	0·07
1, 1, 1	6	−0·21	−0·25	−0·08	−0·17
$\frac{3}{2}$, 1, $\frac{1}{2}$	7	−0·26	−0·25	−0·10	−0·24
$\frac{3}{2}$, $\frac{3}{2}$, 0	8	−0·02	−0·25	−0·15	−0·01
$\frac{3}{2}$, $\frac{3}{2}$, 1	9	−0·37	−0·25	−0·14	−0·25

an octahedral site and its tetrahedral neighbor) implies that the vacant octahedral sites tend to be grouped about occupied tetrahedral sites. The symmetry of the array of superstructure peaks (an example of which is shown in Fig. 1 for those around a 200 $B1$ peak) suggests the appropriate Laue diffraction group is $m3m$. Since no systematic extinctions are present, the ordered structure apparently possesses the point symmetry of $m3m$, $\bar{4}3m$ or 432. Using this information, a specific model for the cation distribution in a $3X$ cell was deduced.

Each complex consisted of 13 vacant octahedral sites (a center site and the twelve nearest neighbor sites around it). A total of 8 tetrahedral sites are included within each vacancy cluster; some or all of these may be occupied by iron ions. One such complex exists on each of the simple cubic lattice points for the $3X$ cell. This model has been chosen with an eye to the concentration of tetrahedral ions, the known composition, and the two positive peaks corresponding to first and second neighbor octahedral sites to any octahedral Fe cation. Within one $3X$ unit of the model there are a total of 108 oxygen ions, 95 octahedral iron ions, and from the previously presented data on structure factor calculations for the $B1$ peaks, about four tetrahedral ions. This corresponds to an overall formula of $Fe_{99}O_{108}$ or $Fe_{0.918}O$, compared to the known composition of $Fe_{0.902}O$; two more vacant cation sites would yield the correct composition. The observed α_i from equation (1) and those from the model are compared in columns 3 and 4 of Table 2.

To make a more direct check whether or not this model really corresponds with the Patterson function found using the observed intensities, Patterson syntheses were made using F^2 calculated from the model for substitutional order. By comparing columns 3 and 5 of Table 2, it can be seen that many of the larger peaks do indeed correspond to the same vectors. The agreement can be improved if the effects of small atom displacements away from the ideal site positions are added to the model (see columns 3 and 6 of Table 2). In the next section, the means of establishing these displacements are discussed in detail.

Structure factor calculations based on the $3x$ cell model

The *ORFLS* computer program with unit weighting was also used in the refinement of the superstructure peaks. One temperature factor was again applied to all iron ions and a second temperature factor to all oxygen ions. Periodically, these two temperature factors and the single scale factor were refined using the *fundamental* peaks alone. These three parameters were then fixed and the other variable parameters refined to give the best agreement with the superstructure intensities measured with Mo $K\alpha$ radiation. Calculations were made using both centrosymmetric and non-centrosymmetric models for the structure. Actually these

Table 3.

Equipoints			Models 1, 2 and 3 Undistorted coordinates			Model 4 Refined coordinates			Parameter range where established [By significance test at $\alpha=0.05$ (95 percent confidence)]
$Pm3m$	$P\bar{4}3m$	Ion	x	y	z	x	y	z	
8(g)	4(e)	Tet. Fe	$\frac{1}{12}$*	$\frac{1}{12}$	$\frac{1}{12}$	0·090	0·090	0·090	$0.57 < n‡ < 1.44$, $0.075 < x < 0.096$
1(a)	1(a)	vacant	0	0	0	0·000	0·000	0·000	
12(i)	12(i)	vacant	$\frac{1}{6}$*	$\frac{1}{6}$	0†	0·166	0·166	0·000	$0.00 < n‡ < 0.03$
6(e)	6(f)	Oct. Fe	$\frac{1}{3}$*	0	0	0·329	0·000	0·000	$0.322 < x < 0.355$
12(i)	12(i)		$\frac{1}{3}$*	$\frac{1}{3}$	0†	0.329_5	0.329_5	0·000	$0.327 < x < 0.332$
12(h)	12(h)		$\frac{1}{2}$	$\frac{1}{6}$*	0	0·500	0·167	0·000	$0.161 < y < 0.170$
24(m)	12(i)		$\frac{1}{3}$*	$\frac{1}{6}$*	$\frac{1}{6}$	0·324	0·158	0·158	$0.321 < x < 0.328$, $0.156 < z < 0.160$
—	12(i)		$-\frac{1}{3}$†	$-\frac{1}{6}$†	$-\frac{1}{6}$	−0·324	−0·158	−0·158	$-0.321 < x < -0.328$, $-0.156 < z < -0.160$
24(l)	24(j)		$\frac{1}{2}$†	$\frac{1}{3}$*	$\frac{1}{6}$*	0·500	0·333	0·167	
8(g)	4(e)		$\frac{1}{3}$*	$\frac{1}{3}$	$\frac{1}{3}$	0·330	0·330	0·330	$0.156 < x < 0.161$
—	4(e)		$-\frac{1}{3}$†	$-\frac{1}{3}$	$-\frac{1}{3}$	−0·330	−0·330	−0·330	$-0.156 < x < -0.161$
6(f)	6(g)		$\frac{1}{2}$	$\frac{1}{2}$	$\frac{1}{3}$*	0·500	0·500	0·333	
3(c)	3(c)		$\frac{1}{2}$	$\frac{1}{2}$	0	0·500	0·500	0·000	
6(e)	6(f)	Oxygen	$\frac{1}{6}$*	0	0	0·172	0·000	0·000	$x < 0.345$
3(d)	3(d)		$\frac{1}{2}$	0	0	0·500	0·000	0·000	
24(k)	24(k)		$\frac{1}{3}$*	$\frac{1}{6}$*	0†	0·338	0·168	0·000	
12(h)	12(h)		$\frac{1}{2}$	$\frac{1}{3}$*	0	0·500	0·333	0·000	
8(g)	4(e)		$\frac{1}{6}$*	$\frac{1}{6}$	$\frac{1}{6}$	0·174	0·174	0·174	
—	4(e)		$-\frac{1}{6}$†	$-\frac{1}{6}$	$-\frac{1}{6}$	−0·174	−0·174	−0·174	
24(m)	12(i)		$\frac{1}{3}$*	$\frac{1}{3}$	$\frac{1}{6}$*	0·338	0·338	0·160	$0.327 < x < 0.344$
—	12(i)		$-\frac{1}{3}$†	$-\frac{1}{3}$	$-\frac{1}{6}$†	−0·338	−0·338	−0·160	
12(j)	12(i)		$\frac{1}{2}$†	$\frac{1}{6}$*	$\frac{1}{6}$	0·500	0·167	0·167	
12(j)	12(i)		$\frac{1}{2}$†	$\frac{1}{3}$*	$\frac{1}{3}$	0·500	0·333	0·333	
1(b)	1(b)		$\frac{1}{2}$	$\frac{1}{2}$	$\frac{1}{2}$	0·500	0·500	0·500	
6(f)	6(g)		$\frac{1}{2}$	$\frac{1}{2}$	$\frac{1}{6}$*	0·500	0·500	0·167	

* Variable in $Pm3m$.
† Additional coordinates variable in $P\bar{4}3m$.
‡ Occupation factor variable between 0 and 1.

two differ only in a minor way (*i.e.* the arrangement of the 4 tetrahedral iron ions in a unit cell) and show essentially the same agreement with the experimental data. Initially all the non-tetrahedral ions were assigned the ideal coordinates listed in Table 3 (Model 1). These ions are centrosymmetric about an origin chosen in the center of a complex and the cell contents are described using the equipoints of the space group $Pm3m$. The 4 tetrahedral ions may be introduced on the eight available sites within each vacancy cluster using an occupation factor of $\frac{1}{2}$ on the 8(g) equipoint of $Pm3m$ (Model 2). As an alternative, the 4 tetrahedral ions may also be introduced on the 4(e) equipoint of $P\bar{4}m3$ (Model 3). This latter possibility seems physically more likely since edge sharing of the coordination polyhedra of the tetrahedral ions would be avoided. In this model, the centrosymmetric arrangement was retained for all but the 4 tetrahedral ions. Attempts to refine the additional coordinates variable in the equipoints of $P\bar{4}3m$ (compared to $Pm3m$) were abandoned since improvement in the 'R values' were small (5 percent) and the model was complicated considerably. The agreement with the observed intensities using Models 2 and 3 was essentially the same. In Model 3, the superstructure peaks surrounding fundamental peaks with odd indices showed an imaginary term 10–20 percent of the

Table 4. *Observed and calculated structure factors*

h	k	l	Mo $K\alpha$ F_{obs}	Co $K\alpha$ F_{obs}	Model 3 F_{calc}	Model 4 F_{calc}
0	0	δ	0·60*		2·67	2·18
0	0	2δ	0·60*		0·47	0·51
0	0	2		(14·1)	45·5	45·7
0	0	$2-2\delta$	0·60*		1·29	1·59
0	0	$2-\delta$	10·95	8·12	5·03	7·77
0	0	$2+\delta$		2·28	4·31	1·14
δ	0	$2-\delta$		3·84	3·61	3·90
δ	0	2		7·07	4·64	4·32
δ	0	$2+\delta$		2·60	3·09	2·54
δ	δ	$2-\delta$		1·51	2·63	2·62
δ	δ	2		3·24	3·33	3·24
δ	δ	$2+\delta$		1·54	2·26	2·26
0	0	$2+2\delta$	0·60*		0·95	0·05
0	0	4		(13·1)	26·2	26·0
0	0	$4-2\delta$	1·51	1·30	0·26	1·03
0	0	$4-\delta$	4·37	3·24	1·32	4·76
0	δ	4	1·75	1·04	1·20	1·37
2δ	0	4		0·84	0·21	0·67
0	0	$4+\delta$	1·73	0·86	1·09	1·78
0	0	$6-\delta$	5·32		1·72	5·16
δ	0	6	2·17		1·58	1·82
0	0	$6+\delta$	1·22		1·46	1·46
0	0	$8-\delta$	2·63		0·47	3·24
δ	0	8	1·22		0·44	0·99
0	0	$8+\delta$	1·22		0·40	1·44
0	0	$10-\delta$	2·98		0·67	3·00
δ	0	10	0·98		0·62	1·01
1	1	1	(8·52)		31·5	31·5
1	1	$1-\delta$	3·94		3·97	5·37
1	$1-\delta$	$1-\delta$	1·34		2·86	3·47
1	1	3	18·9	(8·0)	19·1	19·2
1	1	$3-\delta$	5·59	7·48	2·77	6·48
$1-\delta$	1	3		3·97	2·60	3·62
$1-\delta$	$1-\delta$	3		1·73	1·86	2·05
$1-\delta$	1	$3-\delta$		2·54	1·97	2·69
$1+\delta$	1	3		1·45	2·45	1·23
1	1	$3+\delta$		0·69	2·33	1·58
$1-\delta$	$1+\delta$	3		0·82	1·75	1·74
$1-\delta$	1	$3+\delta$		0·67	1·66	1·26
1	1	5	13·2		11·8	11·8
1	1	$5-\delta$	5·48		1·64	5·47
$1-\delta$	1	5	2·06		1·53	2·23
$1-\delta$	1	$5-\delta$	1·56		1·16	1·69
1	1	7	7·73		7·34	7·32
1	1	$7-\delta$	4·66		1·00	4·39
1	1	9	4·72		4·73	4·70
1	1	$9-\delta$	3·70		0·64	3·46
1	1	11	2·19		2·98	2·95
1	1	$11-\delta$	2.33		0·39	2·54
2	0	2		(14·6)	37·7	37·7

Table 4 (*cont.*)

h	k	l	Mo $K\alpha$ F_{obs}	Co $K\alpha$ F_{obs}	Model 3 F_{calc}	Model 4 F_{calc}
$2-\delta$	0	$2-\delta$		0·56	1·03	0·56
$2-\delta$	0	2		3·04	1·78	3·88
$2-\delta$	0	$2+\delta$		0·76	0·90	1·49
2	δ	2		1·51	1·66	1·61
2	0	4	20·5	(15·3)	21·2	21·2
$2-\delta$	0	$4-\delta$		1·39	1·94	2·62
2	0	$4-\delta$	6·57	5·72	2·58	5·86
2	δ	$4-\delta$		1·58	1·86	1·84
2	δ	4		2·88	2·36	2·44
$2-\delta$	0	4	2·61	4·45	2·47	4·00
$2-\delta$	δ	4		1·29	1·78	1·91
2	0	6	15·0		13·5	13·9
$2-\delta$	0	6	2·26		0·66	1·74
2	0	$6-\delta$	5·89		0·70	3·62
2	0	8	8·79		8·30	8·14
$2-\delta$	0	8	1·93		0·95	1·66
2	0	$8-\delta$	1·11		1·01	3·72
2	2	2	(13·5)		31·6	31·6
2	$2-\delta$	2	6·56		3·32	5·28
2	2	4	18·0		20·2	20·0
$2-\delta$	2	4	1·87		0·97	2·33
$2-\delta$	2	$4-\delta$	0·60*		0·56	0·12
2	2	6	12·3		12·1	12·0
2	2	$6-\delta$	4·13		1·46	4·31
$2-\delta$	2	6	2·08		1·39	2·34
$2-\delta$	2	$6-\delta$	1·14		1·08	0·91
$2-\delta$	$2-\delta$	6	1·87		1·02	1·00
2	2	8	8·56		8·44	8·11
2	2	$8-\delta$	2·28		0·42	2·84
$2-\delta$	2	8	1·39		0·40	1·23
3	1	3	15·2	(8·12)	14·7	14·7
$3-\delta$	1	3		1·54	1·50	1·88
3	$1-\delta$	$3-\delta$		1·14	1·43	1·88
$3-\delta$	1	3	4·14	4·65	2·02	4·67
3	$1-\delta$	3		2·08	1·93	2·70
3	$1+\delta$	3		0·61	1·85	1·15
$3+\delta$	1	$3-\delta$		0·70	1·31	1·87
3	1	5	10·7		9·82	9·90
3	1	$5-\delta$	4·22		1·34	4·39
$3-\delta$	1	5	2·68		1·30	3·01
$3-\delta$	1	$5-\delta$	0·95		0·97	1·12
3	1	7	6·52		6·48	6·53
3	1	$7-\delta$	3·94		0·88	3·76
$3-\delta$	1	7	1·70		0·85	1·94
3	1	9	4·20		4·29	4·35
3	1	$9-\delta$	3·36		0·58	3·03
3	1	11	1·81		2·72	2·77
3	1	$11-\delta$	2·09		0·36	2·27
3	3	3	(10·7)		13·0	13·0
3	$3-\delta$	3	3·31		1·58	3·69
3	3	5	9·11		8·39	8·46
3	3	$5-\delta$	3·54		1·13	3·67
$3-\delta$	3	$5-\delta$	0·87		0·82	0·89
3	3	7	5·87		5·78	5·81
3	3	$7-\delta$	3·40		0·78	3·25
$3-\delta$	3	7	1·53		0·75	1·77
3	3	9	4·07		3·88	3·97
3	3	$9-\delta$	2·75		0·52	2·69

real term. However, the dominating real term was virtually the same for the equipoints of $P\bar{4}3m$ and $Pm3m$ so the calculated amplitudes differed little.

Next, the least-mean-squares program was used to refine the atom positions. Beginning with the ideal packing corresponding to a $B1$ structure, small changes were introduced in the coordinates not fixed by symmetry. The coordinate values found after this refinement are listed in Table 3 (Model 4). Physically, the displacements probably result from electrostatic interactions due to a net negative charge on a vacancy cluster. While displacements from duodecahedral mirror planes (which would lower the symmetry to the equipoints in $P432$) might be present in principle, these were not expected on physical grounds, and were not considered. The difficulties often experienced in refin-

Table 4 (*cont.*)

h	k	l	Mo $K\alpha$ F_{obs}	Co $K\alpha$ F_{obs}	Model 3 F_{calc}	Model 4 F_{calc}
4	0	6	11·94		10·54	10·47
4−δ	0	6	3·11		1·23	2·73
4	0	6−δ	4·14		1·26	3·67
4	0	8	7·61		7·59	7·34
4	0	8−δ	2·34		0·38	2·51
4−δ	0	8	1·64		0·36	1·42
4	0	10	3·41		4·49	4·48
4	0	10−δ	2·15		0·55	2·35
4	2	4	14·3		14·1	14·0
4−δ	2	4	3·78		1·67	3·76
4−δ	2	4−δ	0·75		1·27	0·84
4	2	6	11·3		10·7	10·4
4	2	6−δ	2·13		0·52	2·66
4	2	8	6·49		6·71	6·70
4	2	8−δ	3·09		0·81	2·88
4	2	10	3·97		4·61	4·44
4	4	4	12·0		12·0	11·9
4	4	6	8·4		8·3	8·3
4	4	6−δ	1·66		0·99	2·80
4	4	8−δ	1·96		0·31	1·99
4	4	10	3·2		3·7	3·9
4	4	10−δ	1·25		0·46	1·89
6	0	6	9·01		8·44	8·27
5	1	7	5·31		5·25	5·42
5	1	7−δ	3·76		0·70	2·84
5−δ	1	7	2·02		0·69	2·08
5	1	9	3·36		3·53	3·70
5	1	9−δ	2·54		0·47	2·35
5	3	5	6·83		6·51	6·72
5−δ	3	5	2·33		0·86	2·71
5	3	7	4·88		4·73	4·89
5	3	7−δ	2·81		0·63	2·54
5−δ	3	7	1·94		0·62	1·87
5	3	9	2·89		3·23	3·51
5	5	5	5·16		5·23	5·39
5−δ	5	5	2·02		0·69	2·13
5	5	7	3·67		3·89	4·25
5	5	7−δ	2·03		0·51	1·95
5	5	9	2·48		2·72	2·97
5	5	9−δ	1·45		0·36	1·72
7	1	7	4·08		3·88	4·11
7−δ	1	7	2·25		0·51	1·93
7	1	9	2·33		2·73	3·05
7	1	9−δ	1·56		0·36	1·62
7−δ	1	9	1·04		0·35	1·18
7	3	7	3·25		3·55	3·89
7−δ	3	7	1·66		0·46	1·71
7	5	7	2·80		2·96	3·24
7−δ	5	7	1·24		0·38	1·45
7	5−δ	7	0·81		0·38	1·15
					$B_{Fe}=0·67$ Å^2	$B_{Fe}=0·45$ Å^2
					$B_0=0·79$ Å^2	$B_0=0·75$ Å^2

* The reflections were not detected although they were looked for, and are assigned the estimated minimum observable value of F. They were not included in the refinement but are included in R values. Values in parantheses are probably affected by extinction.

R' values	Mo $K\alpha$ Fundamental peaks	Mo $K\alpha$ Supplemental peaks	Mo $K\alpha$ All peaks	Co $K\alpha$ Supplemental peaks
Model 3 (Substitution only)	0·054	0·620	0·252	0·433
Model 4 (both displacement and substitution)	0·062	0·157	0·095	0·247

ing a highly symmetric structure with the linear least-squares method were severe. A singular matrix was obtained from the normal equations if ideal coordinates were used in the first cycle; it was thus necessary first to introduce small distortions rather arbitrarily. Even after doing this, unreasonable and rapidly diverging parameter changes were often encountered. This was circumvented by several cycles of refinement,

with a shift factor of 0·20. Some changes in parameters were highly correlated. Particular problems were encountered with some of the oxygen ions.

The 'R' value' for the Mo $K\alpha$ superstructure peaks was reduced from 0·620 (for Model 3 where no displacements were considered) to 0·157 with displacements, and the overall R' value was 0·095. An investigation of the behavior of the R values in the vicinity of the supposed best parameter values was then made. For many parameters, there was a sufficiently pronounced minimum in R'' to define a range of values by a significance test at the level $\alpha=0{\cdot}05$ (95 percent confidence level); these ranges are shown in Table 3. It should be kept in mind, however, that in view of the correlations in some coordinates, the significance test is only an approximation.

The various stages of the refinement are indicated at the bottom of Table 4. Note particularly that static displacements contribute to the peak depression (that is they are part of the term modifying the atomic form factor, $\exp[-2B\sin^2\theta/\lambda^2]$), until these are 'removed' in Model 4 by including them as displacements in the atomic coordinates. Table 4 presents F_{obs} for all peaks and also F_{cal} for Models 3 and 4. In addition to being highly asymmetric in intensity around each fundamental, observed superstructure reflections increased in intensity relative to the fundamental peaks with increasing distance from the origin of reciprocal space, but with some oscillation, being higher for peaks near fundamental reflections for which $h+k+l=4n+2$ and lower for $h+k+l=4n$. This is just the opposite to the predicted effect of tetrahedral ions on the neighboring fundamental peaks, and indeed just such an oscillation appeared in the calculated structure factors for Model 3, which included tetrahedral occupation but not displacements. (The oscillation is, of course, also observed with displacements, Model 4.)

Discussion

This study has demonstrated that the defects present in $Fe_{1-x}O$ are clusters of vacancies containing tetrahedral iron cations, the clusters being arranged periodically only in specimens quenched to room temperature. The final structure is shown in Fig. 6. The clusters are *not* small spinel regions although they have some resemblance to them. To check this point, the difference Patterson function for Fe_3O_4 was calculated. The peaks representing first and second neighbors were positive and negative respectively, whereas in Fig. 5(*a*) these are positive. These would not be present for stoichiometric FeO. Thus any distribution of cells of Fe_3O_4 in $Fe_{1-x}O$ must lead to a negative value for the second-neighbor peak. In fact, we have been unable to find any periodic arrangement involving FeO and Fe_3O_4 that would satisfy the composition $Fe_{0{\cdot}902}O$ and maintain cubic symmetry. The precise number of vacancies and tetrahedral cations in each cluster is not closely defined in the present work, although substantial agreement with the observed intensities can be achieved for $Fe_{0{\cdot}902}O$ with a cluster of 13 octahedral vacancies and 4 tetrahedral ions. Displacements of the other ions around each cluster occur, probably as a result of electrostatic interactions. The bond lengths were calculated for the coordinates of Model 4. The shortest bond is between a tetrahedral ion and its 4 oxygen near neighbors. Three of these are at 1·94 Å and the fourth is at 1·87 Å whereas in Fe_3O_4 all four are at 1·87 Å. The bond distance between an octahedral iron ion and its anion neighbors ranges from 2·02 Å to 2·31 Å. These may be compared with the value of 2·06 Å for such pairs in Fe_3O_4. The distortions destroy perfect octahedral and tetrahedral coordination of all the cations; this may be the reason for the quadrupole splitting observed in Mössbauer patterns (Shirane, Cox & Ruby, 1962; Hillman, 1965.)

Whether or not interstitial occupation varies at temperature with composition is not certain, although it is known to do so in quenched specimens (Roth, 1960; Smuts, 1966). The peculiar effect of tetrahedral ions on the extra peaks could be used to study this as a function of both temperature and composition. Such work is contemplated, as it might shed light on the unusual phase regions reported by Raccah & Vallet (1965) and might also clarify the changes with temperature of the partial pressure dependence of vacancy concentration and conductivity. It is clear that vacancies are clustered even at temperatures and compositions where the first thoughts about the results concerning these properties suggest that there are *no* deviations from randomness.

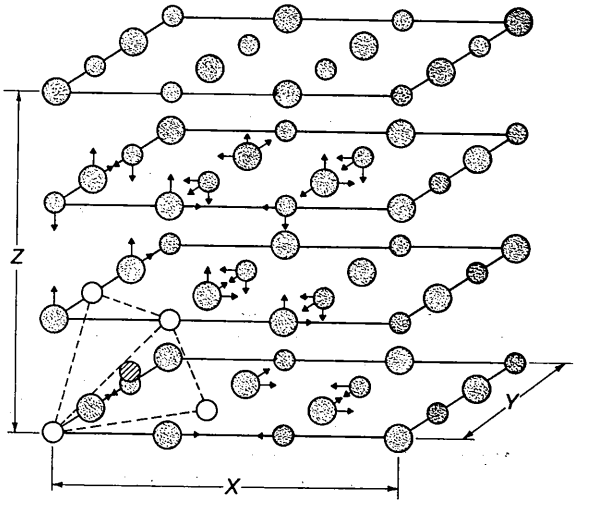

Fig. 6. One octant of the $3X$ unit cell. Open circles represent octahedral vacancies, shaded circle one of the four tetrahedral iron ions associated with a cluster. The components of displacement found for the ions surrounding the vacancy complex are indicated by arrows, with large and small filled circles representing oxygen and octahedral iron ions respectively .

There is some difficulty in estimating the Debye temperature of $Fe_{1-x}O$ from data on its specific heat, because of its anti-ferromagnetic transition (Todd & Bonnickson, 1951). From the values of B in Model 4, for which the static displacements have been effectively removed, a value of 540°K is calculated, after an approximate correction for thermal diffuse scattering (Chipman & Paskin, 1959).

This work was started by one of the authors (F. K.) as part of a class project in an advanced diffraction course given by J. B. C. at Northwestern University, and was continued as a Ph. D. thesis supported by the Air Force Office of Scientific Research, Office of Aerospace Research, U. S. Air Force, through AF Grant No. 327–63. Stimulating discussions with Professor M. E. Fine (who supervised other portions of the thesis) are gratefully acknowledged. We also wish to thank Professor J. Ibers and Dr P. Corfield for the use of their computer programs for Fourier syntheses, discussions on their application, and for their version of the Busing–Martin–Levy least-mean-squares program. Professor J. B. Wagner, Jr. kindly supplied us with the single-crystal specimen, and Mr J. Gragg first directed our attention to the form of equation (1). Partial support by ARPA, and by NSF through Northwestern University's Vogelback Computing Center, is also appreciated.

References

BERTAUT, E. F. (1953). *Acta Cryst.* **6**, 557.
BRANSKY, I. & TANNHAUSER, D. (1967). *Trans. Amer. Inst. Min. (Metall.) Engrs.* **239**, 75.
BRYNESTAD, J. & FLOOD, H. (1958). *Z. Electrochem.* **62**, 953.
BUSING, W. R., MARTIN, K. O. & LEVY, H. A. (1960). *ORFLS, Program* described in Oak Ridge Nat. Lab. Rept. TM-305; modified by Ibers, J. A. (1965).
CHIPMAN, D. R. & PASKIN, A. (1959). *J. Appl. Phys.* **30**, 1998.
COOPER, M. J. (1963). *Acta Cryst.* **16**, 1067.
COWLEY, J. M. (1960). *Phys. Rev.* **120**, 1648.
CRUICKSHANK, D. W. J. (1965). *Computing Methods in Crystallography*, p.114, Ed. J. S. ROLLETT. New York: Pergamon Press.
DARKEN, L. S. & GURRY, R. W. (1945). *J. Amer. Chem. Soc.* **67**, 1398.
FRUEH, A. J. (1953). *Acta Cryst.* **6**, 454.
FUJIWARA, K. (1957). *J. Phys. Soc. Japan*, **12**, 7.
GATINEAU, L. (1964). *Bull. Soc. Franç. Minér. Crist.* **87**, 321.
GUINIER, A. (1963). *X-ray Diffraction in Crystals, Imperfect Crystals, and Amorphous Bodies*, p.279. New York: Freeman.
HAMILTON, W. (1965). *Acta Cryst.* **18**, 502.
HEMBREE, P. & WAGNER, J. B. (1966). Private communication.
HILLMAN, P. (1965). A. F. Rept. No. 61(052)-62.
HUMPHREY, G. L., KING, E. G. & KELLEY, K. K. (1952). U. S. Bureau of Mines Rept. 4870.
JETTE, E. R. & FOOTE, F. (1933). *J. Chem. Phys.* **1**, 29.
KOCH, F. B. (1967). Ph. D. Thesis, Northwestern University.
KOCH, F. B. & FINE, M. F. (1966). *J. Appl. Phys.* **38**, 1470.
LEVIN, R. L. & WAGNER, J. B. (196). *Trans. Amer. Inst. Min. (Metall.) Engrs.* **236**, 517.
MANENC, J. (1963*a*). *J. Phys. Radium*, **24**, 447.
MANENC, J., BOURGEOT, J., & BENARD, J. (1963*b*). *C. R. Acad. Sci. Paris*, **256**, 931.
MANENC, J., HERAI, T., THOMAS, B. & BENARD, J. (1964). *C. R. Acad. Sci. Paris*, **258**, 4528.
RACCAH, P. & VALLET, P. (1965). *Mem. Sci. Rev. Met.* **62**, 1.
ROTH, W. L. (1959). *J. Appl. Phys.* **30**, 3035.
ROTH, W. L. (1960). *Acta Cryst.* **13**, 140.
SALMON, O. N. (1961). *J. Phys. Chem.* **65**, 550.
SCHWARTZ, L. H., MORRISON, L. A. & COHEN, J. B. (1964). *Advanc. X-Ray Anal.* Vol.7. New York: Plenum Press.
SHIRANE, G., COX, D. E. & RUBY, S. L. (1962). *Phys. Rev.* **125**, 1158.
SMUTS, J. (1966). *J. Iron St. Inst.* **204**, 237.
SWAROOP, B. & WAGNER, J. B. (1967). *Trans. Met. Soc. Amer. Inst. Min. (Metall.) Engrs.* **239**, 1215.
TAKONOMI, M. (1965). *Acta Cryst.* **19**, 486.
TODD, S. S. & BONNICKSON, K. R. (1951). *J. Amer. Chem. Soc.* **73**, 3894.
WYCKOFF, R. W. G. & CRITTENDEN, E. D. (1925). *J. Amer. Chem. Soc.* **47**, 2876.